

# Transmission analysis of long-period fiber grating with trapezoid index modulation

GUO-DONG WANG, CAI-XIA LIU, DONG-MING SUN, WEN-BIN GUO, WEI-YOU CHEN\*

College of Electronic Science and Engineering, State Key Laboratory on Integrated Optoelectronics, Jilin University, 2699 Qianjin Street, Chang chun, 130012, China.

\*Corresponding author: Wei-You Chen, quantumwgd@yahoo.com.cn

The long-period fiber grating (LPG) with trapezoid index modulation is presented as a novel grating. The influence of the difference between the top width and the bottom width (simplified to  $d$  in the following text) of the trapezoid index modulation on the transmission characteristics is analyzed. Calculated results show that the resonance location displaces to the long wavelength when the  $d$  increases. Compared with the long-period fiber grating with rectangle index modulation, the advantage of this novel grating is that it needs a smaller refractive index change. When  $d$  is zero, this model can be used to simulate the LPG with a rectangular index modulation, and the theoretical results are in good agreement with the experimental ones.

Keywords: long-period fiber grating, trapezoid index modulation, transmission spectrum.

## 1. Introduction

The long-period fiber grating (LPG) is a transmission-type notch filter. By using this device, optical power can be coupled from the fundamental core mode to the phase-matched cladding modes [1, 2]. It has a wide variety of applications, such as gain flattening of erbium-doped fiber amplifiers [3], multi-channel filtering [4], wavelength division multiplexing communication system [5], dispersion compensation [6, 7], and temperature, strain and refractive index sensing [8–12].

There is a refractive index modulation for fiber Bragg grating or LPG. Based on the perturbation theory, the refractive index modulation can be considered as a perturbation of the fiber core refractive index. In the initially theoretical model of the grating, the perturbation can be regarded as a sinusoidal function [1, 2]. This model can accurately simulate the spectrum property of the Bragg grating and the LPG that are fabricated by the phase mask method. However, for the LPG fabricated with the amplitude mask method, the perturbation is a rectangular index modulation (RIM) [13, 14]. Some errors would appear if we computed the spectrum property of LPG with

RIM with the sinusoidal model. Therefore, a LPG model with RIM was proposed for avoiding the mistakes caused by the initial model [14].

In this paper, a novel model of LPG is presented, which has a trapezoid index modulation (TIM). The coupling interactions considered in this new model include not only the coupling between the fundamental core mode and the cladding modes, but also the self-coupling of the cladding modes. The material dispersion of fiber is considered in the simulation. The advantage of the LPG with TIM is that it can deduce the refractive index change. When the  $d$  of TIM is equal to zero, the LPG with TIM is transformed to the LPG with RIM. In this case, the LPG with TIM model can be used to simulate the LPG with RIM. Calculation shows that theoretical results agree with the experimental ones.

This paper is organized as follows. In Section 2, we present the refractive index distribution in the LPG with TIM. Then in Section 3, based on the coupled-mode theory, the formulae of coupling coefficients and coupled-mode equations are derived for the LPG with TIM. Furthermore in Section 4, we perform the analysis of the effects on the grating transmission spectrum, including the difference between the top width and the bottom width of TIM. Finally, conclusions are drawn in Section 5.

## 2. Refractive index distributing in TIM-LPG

The fiber considered in this paper has a step-index profile and a three-layer structure. The three-layer structure comprises a core, a cladding and air. The parameters of the fiber are as follows: the core radius  $a_1 = 2.5 \mu\text{m}$ , cladding radius  $a_2 = 62.5 \mu\text{m}$ , index difference  $\Delta = (n_1^2 - n_2^2)/2n_1^2 = 0.45\%$ , where  $n_1$  is the core index and  $n_2$  is the cladding index. The air index is 1. The material dispersion must be considered when the range of wavelength during the process of calculation is very large (for example,  $0.9\text{--}1.6 \mu\text{m}$ ). The material dispersion equations we considered in this paper are the same as those in [14].

The refractive index distribution in the fiber core of the LPG with TIM is illustrated in Fig. 1, and can be expressed as:

$$n_1(z) = n_1 \left[ 1 + \sigma(z)f(z) \right] \quad (1)$$

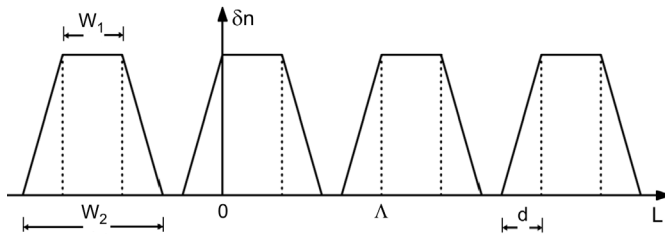


Fig. 1. Trapezoid index modulation in the fiber core.

where  $\sigma(z)$  is the apodization, and  $f(z)$  is the trapezoid function given by:

$$f(z) = \begin{cases} 1 & (2n-1)\Lambda \leq z < 2n\Lambda - (1-p)\Lambda \\ \frac{z + (1-p)\Lambda - d}{-d} & 2n\Lambda - (1-p)\Lambda \leq z < 2n\Lambda - (1-p)\Lambda + d \\ 0 & 2n\Lambda - (1-p)\Lambda + d \leq z < 2n\Lambda - d \\ \frac{z + d}{d} & 2n\Lambda - d \leq z < 2n\Lambda \\ 1 & 2n\Lambda \leq z < (2n+p)\Lambda \\ \frac{z - p\Lambda - d}{-d} & (2n+p)\Lambda \leq z < (2n+p)\Lambda + d \\ 0 & (2n+p)\Lambda + d \leq z < (2n+1)\Lambda - d \\ \frac{z + d - \Lambda}{d} & (2n+1)\Lambda - d \leq z < (2n+1)\Lambda \end{cases} \quad (2)$$

where  $n = 0, 1, 2, 3, \dots, N$  ( $N$  is the number of the period along the grating length),  $\Lambda$  is the grating period,  $p = W_1/\Lambda$  and  $d$  is defined as  $d = (W_2 - W_1)/2$  ( $W_1$  is the top width of TIM and  $W_2$  is the bottom width of TIM). The grating length is  $L = N\Lambda$ .

Expanding Eq. (2) to the Fourier series, we have

$$f(z) = a_0 + \sum_{j=1}^{\infty} \sqrt{a_j^2 + b_j^2} \cos\left(\frac{2j\pi}{\Lambda} z - \theta_j\right) \quad (3)$$

with

$$a_0 = p + \frac{d}{\Lambda} \quad (4a)$$

$$a_j = \frac{\Lambda}{2j^2\pi^2d} \left[ 1 + \cos(2jp\pi) - \cos\left(\frac{2jd\pi}{\Lambda}\right) - \cos\left(2jp\pi + \frac{2jd\pi}{\Lambda}\right) \right] \quad (4b)$$

$$b_j = \frac{\Lambda}{2j^2\pi^2d} \left[ \sin(2jp\pi) + \sin\left(\frac{2jd\pi}{\Lambda}\right) - \sin\left(2jp\pi + \frac{2jd\pi}{\Lambda}\right) \right] \quad (4c)$$

$$\theta_j = \arcsin\left(\frac{b_j}{\sqrt{a_j^2 + b_j^2}}\right) \quad (4d)$$

where  $j = 1, 2, 3, \dots$ . Substituting Eqs. (3) and (4) into Eq. (1), we can express the refractive index distribution in the fiber core as

$$n_1(z) = n_1 + n_1 \sigma(z) \left\{ \frac{d}{\Lambda} + p \left[ 1 + \sum_{j=1}^{\infty} m_j \cos \left( \frac{2j\pi}{\Lambda_j} z - \theta_j \right) \right] \right\} \quad (5)$$

and then we obtain

$$\delta n_1(z) = n_1 \sigma(z) \left\{ \frac{d}{\Lambda} + p \left[ 1 + \sum_{j=1}^{\infty} m_j \cos \left( \frac{2j\pi}{\Lambda_j} z - \theta_j \right) \right] \right\} = n_1 \sigma(z) f(z) \quad (6)$$

The mode fields in the single mode fiber are composed of by the core mode, the cladding modes and the radiation modes. The expressions for these mode fields can be found in some previous papers [1, 2].

### 3. Coupling coefficient and coupled-mode function

The transverse coupling coefficient  $K_{\nu\mu}^t$  between modes  $j$  and  $k$  is given by [1, 2]

$$K_{\nu\mu}^t = \frac{\omega}{4} \int_0^{2\pi} d\varphi \int_0^{\infty} r dr \Delta \varepsilon E_{\nu}^t E_{\mu}^{t*} \quad (7)$$

since  $\delta n_{\text{co}}$  is small enough (generally,  $10^{-4} \sim 10^{-3}$ ), we can make the approximation

$$\Delta \varepsilon \cong \varepsilon_0 \Delta(n^2) = 2 \varepsilon_0 n_{\text{co}} \delta n_{\text{co}} = 2 \varepsilon_0 n_{\text{co}}^2 \sigma(z) f(z) \quad (8)$$

We further define the coupling constant as

$$k_{\nu\mu} = \omega \pi \varepsilon_0 n_{\text{co}}^2 \sigma(z) p \int_0^{\infty} r dr E_{\nu} E_{\mu} \quad (9)$$

By substituting Eqs. (3) and (8) into Eq. (7), the transverse coupling coefficient is given by:

$$K_{\nu\mu}^t = k_{\nu\mu} \left[ 1 + \frac{d}{\Lambda p} + \sum_{j=1}^{\infty} m_j \cos \left( \frac{2\pi}{\Lambda_j} z - \theta_j \right) \right] \quad (10)$$

Then, substituting the field expression of the core mode and the cladding modes into Eq. (9), the coupling constant between different modes can be written as

$$k_{01-01}^{\text{co-co}} = \sigma(z) \frac{2\pi}{\lambda} \frac{n_{\text{co}}^2 b p}{n_{\text{cl}} \sqrt{1+2b\Delta}} \left[ 1 + \frac{J_0^2(V\sqrt{1-b})}{J_1^2(V\sqrt{1-b})} \right] \quad (11)$$

$$k_{1\nu-01}^{\text{cl-co}} = \sigma(z) p \frac{2\pi}{\lambda} \left( \frac{\pi b}{Z_0 n_{\text{cl}} \sqrt{1+2b\Delta}} \right)^{1/2} \frac{n_{\text{co}}^2 u_1}{u_1^2 - V^2(1-b)/a_1^2} \\ \times \left( 1 + \frac{\sigma_2 \zeta_0}{n_1^2} \right) E_{1\nu}^{\text{cl}} \left[ u_1 J_1(u_1 a_1) \times \frac{J_0(V\sqrt{1-b})}{J_1(V\sqrt{1-b})} - \frac{V\sqrt{1-b}}{a_1} J_0(u_1 a_1) \right] \quad (12)$$

$$k_{1\nu-1\nu}^{\text{cl-cl}} = \frac{2\pi\lambda}{c} \varepsilon_0 n_{\text{co}}^2 \sigma(z) p \int_0^\infty r dr E_\nu^2 \quad (13)$$

with  $b$ ,  $\Delta$ ,  $V$ ,  $u_1$ ,  $\sigma_2$  and  $\zeta_0$  being defined in [1].

According to the coupled-mode theory, the general coupled-mode equations can be written as [1]

$$\frac{dA_\mu}{dz} = i \sum_\nu A_\nu \left( K_{\nu\mu}^t + K_{\nu\mu}^z \right) \exp \left[ i(\beta_\nu - \beta_\mu)z \right] \\ + i \sum_\nu B_\nu \left( K_{\nu\mu}^t - K_{\nu\mu}^z \right) \exp \left[ -i(\beta_\nu + \beta_\mu)z \right] \quad (14a)$$

$$\frac{dB_\mu}{dz} = -i \sum_\nu A_\nu \left( K_{\nu\mu}^t - K_{\nu\mu}^z \right) \exp \left[ i(\beta_\nu - \beta_\mu)z \right] \\ - i \sum_\nu B_\nu \left( K_{\nu\mu}^t + K_{\nu\mu}^z \right) \exp \left[ -i(\beta_\nu + \beta_\mu)z \right] \quad (14b)$$

where  $A_\mu$  and  $B_\mu$  are the amplitudes for the transverse mode field traveling to the right (+ $z$  direction) and to the left ( $-z$  direction), respectively,  $\beta_\nu$  and  $\beta_\mu$  are the propagation constants of these modes and  $K_{\nu\mu}^z$  is the longitudinal coupling coefficient between modes  $\nu$  and  $\mu$ .

Since the longitudinal coupling coefficients  $K_{\nu\mu}^z$  are substantially smaller than the transverse coupling coefficients  $K_{\nu\mu}^t$  [1], we neglect the  $K_{\nu\mu}^z$  in Eqs. (14). Furthermore, the coupling interactions in the LPG mainly exist between the co-propagating modes, so we disregard the influence of the counter-propagating modes. It is well known that  $k_{1\nu-1\mu}^{\text{cl-cl}} \ll k_{1\nu-01}^{\text{cl-co}} \ll k_{01-01}^{\text{co-co}}$ , so we can ignore the coupling between the different cladding modes. Therefore, the main coupling interactions in the LPG with TIM include the self-coupling of the core mode  $\text{LP}_{01}$ , self-coupling of

the cladding modes  $HE_{1\nu}$ , and coupling of the core mode to the cladding modes. Finally, by using the synchronous approximation, Eqs. (14) is simplified to

$$\frac{dA^{\text{co}}}{dz} = ik_{01-01}^{\text{co-co}} A^{\text{co}} \left(1 + \frac{d}{\Lambda p}\right) + \frac{i}{2} \sum_{\nu} \left\{ k_{1\nu-01}^{\text{cl-co}} A_{\nu}^{\text{cl}} \sum_{j=1}^{\infty} [m_j \exp(-i \delta_{\nu,j} z)] \right\} \quad (15)$$

$$\sum_{\nu} \left\{ \frac{dA_{\nu}^{\text{cl}}}{dz} = ik_{1\nu-1\nu}^{\text{cl-cl}} A_{\nu}^{\text{cl}} \frac{d}{\Lambda p} + ik_{1\nu-01}^{\text{co-co}} A^{\text{co}} \sum_{j=1}^{\infty} [m_j \exp(i \delta_{\nu,j} z)] \right\} \quad (16)$$

$$\delta_{\nu,j} = \beta_{01}^{\text{co}} - \beta_{1\nu}^{\text{cl}} - \frac{2\pi}{\Lambda_j} \quad (j = 1, 2, 3, \dots) \quad (17)$$

where  $A^{\text{co}}$  is the amplitude for the core mode  $LP_{01}$ , and  $A_{\nu}^{\text{cl}}$  is the amplitude for the cladding mode  $HE_{1\nu}$ . Compared with the coupled-mode equations of the LPG with RIM (Eqs. (30) and (31) in [15]), Eqs. (15) and (16) have the additional items  $i \frac{d}{\Lambda p} k_{01-01}^{\text{co-co}} A^{\text{co}}$  and  $i \frac{d}{\Lambda p} k_{1\nu-1\nu}^{\text{cl-cl}} A_{\nu}^{\text{cl}}$ , respectively.

The boundary conditions of the TIM-LPG with length  $L$  are

$$\begin{aligned} A^{\text{co}}(z=0) &= 1 \\ A_{1\nu}^{\text{cl}}(z=0) &= 0 \end{aligned} \quad (18)$$

The transmission rate of this grating can be written as

$$\rho = \frac{|A^{\text{co}}(z=L)|^2}{|A^{\text{co}}(z=0)|^2} \quad (19)$$

In order to get the transmission spectrum of the TIM-LPG, a numerical solution of Eq. (14) is necessary. The fourth-order, adaptive-step-size Runge–Kutta algorithm subject to the boundary conditions is sufficient and accurate.

#### 4. Calculation and discussion

In this section, we investigate the transmission spectrum of the LPG with TIM when the TIM parameter  $d$  has different value.

Figure 2 shows a theoretical calculation of the transmission of the LPG with TIM. The grating parameters are given as follows:  $\Lambda = 250 \mu\text{m}$ ,  $L = 7.6 \text{ mm}$ ,  $\Delta n = 1.26 \times 10^{-3}$ ,  $p = 0.5$  and  $d = 20 \mu\text{m}$ . The six main dips in the spectrum correspond to the core mode coupling to the cladding modes of  $\nu = 5, 7, 9, 11, 13, 15$ .

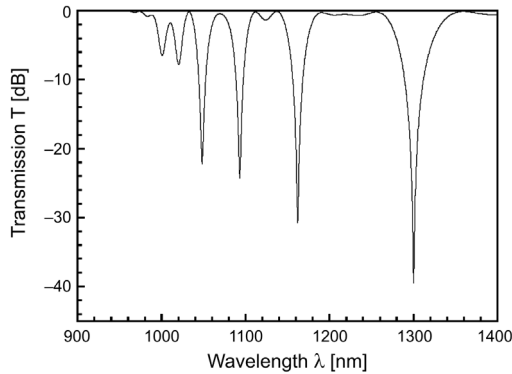


Fig. 2. Transmission spectra of the LPG with TIM, where  $A = 250 \mu\text{m}$ ,  $L = 7600 \text{ mm}$ ,  $\Delta n = 1.26 \times 10^{-3}$ ,  $p = 0.5$  and  $d = 20 \mu\text{m}$ .

We investigate the resonance wavelength as a function of the  $d$  of TIM, as illustrated in Fig. 3. The grating parameters are the same as those in Fig. 2. From Fig. 3, we can conclude that the resonance wavelength displaces to the long wavelength as  $d$  increases. For example, the resonance wavelength between the  $LP_{01}$  mode and the  $HE_{1,15}$  mode displaces from 1298.2 to 1311.4 nm when  $d$  increases from 10 to 25 nm.

From Eq. (10), we can see that the transverse coupling coefficient  $K_{\nu\mu}^t$  increases with an increase of the parameter  $d$ . The resonance strength, which is brought about by the coupling between the core mode and cladding modes, becomes stronger when the transverse coupling coefficient increases, and more power of the core mode is transferred to the cladding mode. So, the transmission dips increase with an increase of parameter  $d$ . When the value of parameter  $d$  is great enough, the power of the core mode is fully transferred to the cladding mode. In this case, the power begins to transfer

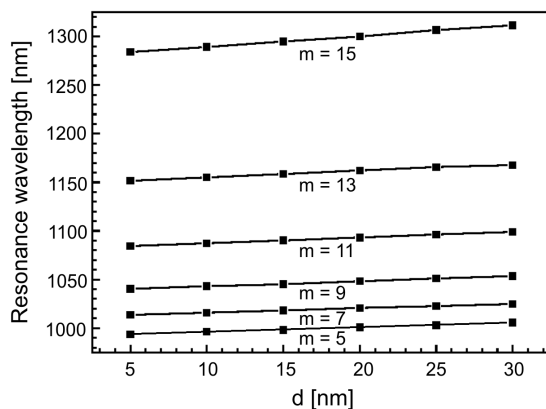


Fig. 3. Resonance wavelength as a function of parameter  $d$ , where  $m$  denote the order of the  $l = 1$  cladding modes.

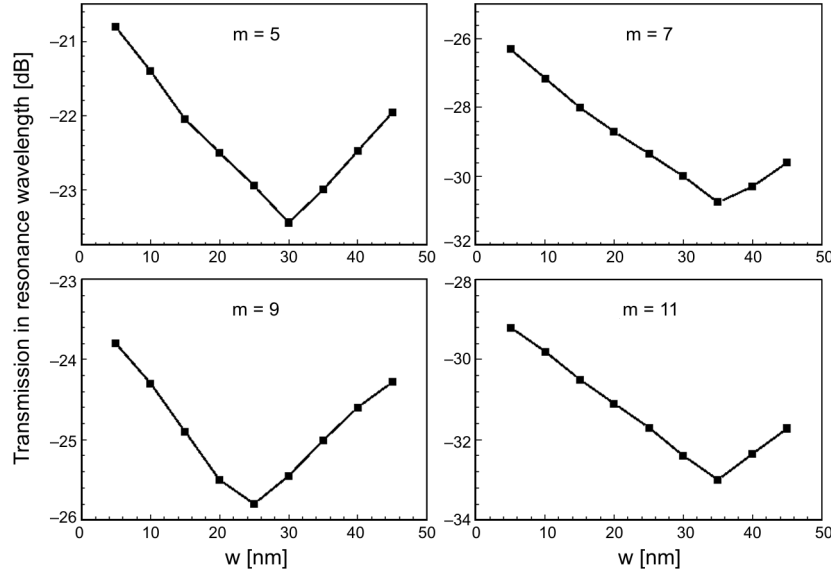


Fig. 4. Transmission dip in resonance wavelength as a function of  $d$ , where  $m$  denote the order of the  $l = 1$  cladding modes.

back from the cladding modes to the core mode when the parameter  $d$  keeps on increasing. The final result is that the transmission dips become weaker when the  $d$  increases. The curves of transmission dips as a function of parameter  $d$  are illustrated in Fig. 4.

Compared to the LPG with RIM, the advantage of the LPG with TIM is that it needs a smaller refractive index change  $\Delta n$  for the same resonance location and strength. For example, the refractive index change as a function of  $d$  is illustrated in Fig. 5, in which the coupling appears between the core mode and cladding mode of  $\nu = 13$ . The resonance location is at  $\lambda = 1.148 \mu\text{m}$  and the resonance dip strength is  $-29.2 \text{ dB}$ . The grating parameters are the same as those in Fig. 2. For the LPG with RIM, the value of the refractive index change is  $1.26 \times 10^{-3}$ , but for the LPG with TIM, it could be obviously deduced. For instance, when  $d = 30 \mu\text{m}$ , the value of  $\Delta n$  is  $1.01 \times 10^{-3}$ , which is only 80.2% of the LPG with RIM.

We notice that if  $d = 0$ , the trapezoid index modulation in Fig. 1 will convert to the rectangle index modulation. In this case, the LPG model with a TIM can be used to simulate the long period grating with RIM. Using this method, we calculate a long period grating transmission spectrum. The results are illustrated in Fig. 6 (dashed line). The solid line in Fig. 6 (*cf.*, Fig. 7 in [15]) is the measured transmission spectrum of a long period grating with the same parameters. The grating parameters in our calculation are listed as  $\Lambda = 1.98 \mu\text{m}$ ,  $L = 7.6 \text{ mm}$ ,  $\Delta n = 1.26 \times 10^{-3}$ ,  $p = 0.5$  and  $d = 0$ . Comparing the solid and dashed lines in Fig. 6, we can conclude that the theoretical results match the experimental results mutually. The theoretical resonance wavelengths

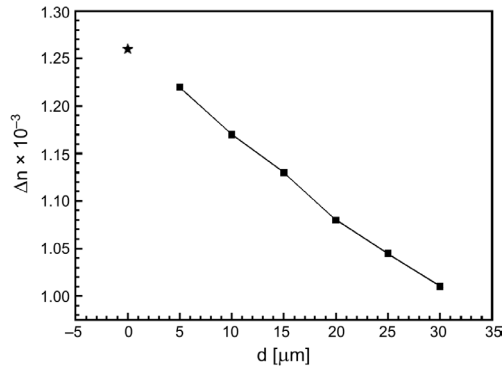


Fig. 5. Refractive index change as a function of parameter  $d$ , where ★ denotes the LPG with RIM and ■ denotes the LPG with TIM.

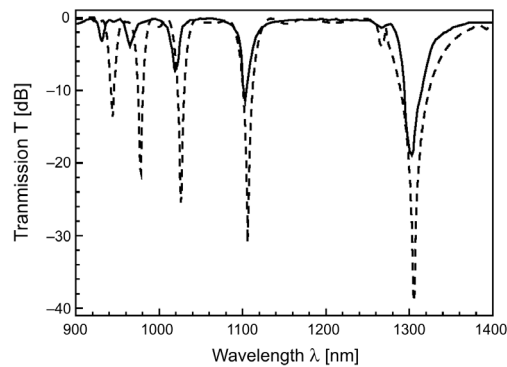


Fig. 6. Theoretically calculated (dashed line) and experimental (solid line) transmission spectra of a LPG with RIM.

are 944, 978, 1024, 1106, 1267 and 1306 nm, respectively; and the experimental resonance wavelengths are 930, 965, 1020, 1104, 1267 and 1306 nm. But the strength of transmission dips is stronger in theory than that found in experiment. The reason is that because of the limited slit function of optical spectrum analyzer, the lowest point of the transmission spectra cannot be measured.

## 5. Conclusions

In this paper, a new type long period grating with a trapezoid index modulation has been presented. A theoretical method has been proposed for analyzing the spectral characteristics of the novel grating presented. The calculated results show that the resonance location displaces to the long wavelength when the  $d$  of TIM increases. Compared with the LPG with RIM, the LPG with TIM needs a smaller refractive index

modulation for the same coupling degree. Furthermore, when  $w = 0$ , the grating model can be used to simulate the long period grating spectra with a RIM, and the theoretical results are in good agreement with the experimental ones.

*Acknowledgment* – This work was supported by the Program of the National Natural Science Foundation of China (Grant No. 69937010) and the Foundation for Outstanding Young Scholars of Jilin Province, China (Grant No. 20005504).

## References

- [1] ERDOGAN T., *Cladding-mode resonances in short- and long-period fiber grating filters*, Journal of the Optical Society of America A: Optics, Image Science and Vision **14**(8), 1997, pp. 1760–73.
- [2] ERDOGAN T., *Fiber grating spectra*, Journal of Lightwave Technology **15**(8), 1997, pp. 1277–94.
- [3] CHO J.Y., LEE K.S., *PDL-compensated mechanically induced long-period grating for EDFA gain flattening*, Fiber and Integrated Optics **23**(6), 2004, pp. 447–51.
- [4] HARUMOTO M., SHIGEHARA M., KAKUI M., KANAMORI H., NISHIMURA M., *Compact long-period grating module with multi-attenuation peaks*, Electronics Letters **36**(6), 2000, pp. 512–4.
- [5] DAS M., THYAGARAJAN K., *Wavelength-division multiplexing isolation filter using concatenated chirped long period gratings*, Optics Communications **197**(1–3), 2001, pp. 67–71.
- [6] DAS M., THYAGARAJAN K., *Dispersion compensation in transmission using uniform long period fiber gratings*, Optics Communications **190**(1–6), 2001, pp. 159–63.
- [7] AIPING LUO, KAN GAO, FENG LIU, RONGHUI QU, ZUIJIE FANG, *Evanescence-field coupling based on long period grating and tapered fiber*, Optics Communications **240**(1–3), 2004, pp. 69–73.
- [8] LEE S.T., KUMAR R.D., KUMAR P.S., RADHAKRISHNAN P., VALLABHAN C.P.G., NAMPOORI V.P.N., *Long period gratings in multimode optical fibers: application in chemical sensing*, Optics Communications **224**(4–6), 2003, pp. 237–41.
- [9] ALLSOP T., WEBB D.J., BENNION I., *A comparison of the sensing characteristics of long period gratings written in three different types of fiber*, Optical Fiber Technology: Materials, Devices and Systems **9**(4), 2003, pp. 210–23.
- [10] FALCIAI R., MIGNANI A.G., VANNINI A., *Long period gratings as solution concentration sensors*, Sensors and Actuators B: Chemical **74**(1–3), 2001, pp. 74–7.
- [11] SHIZHUO YIN, KUN-WOOK CHUNG, XIN ZHU, *A highly sensitive long period grating based tunable filter using a unique double-cladding layer structure*, Optics Communications **188**(5–6), 2001, pp. 301–5.
- [12] KEITH J., PUCKETT S., PACEY G.E., *Investigation of the fundamental behavior of long-period grating sensors*, Talanta **61**(4), 2003, pp. 417–21.
- [13] BAI-OU GUAN, A-PING ZHANG, HWA-YAW TAM, CHAN H.L.W., CHUNG-LOONG CHOY, XIAO-MING TAO, DEMOKAN M.S., *Step-changed long-period fiber gratings*, IEEE Photonics Technology Letters **14**(5), 2002, pp. 657–9.
- [14] XIN-HUA XU, YI-PING CUI, *Theoretical analysis and numerical calculation for the transmission spectrum of long-period fiber gratings with a rectangular index modulation*, Acta Physica Sinica **52**(1), 2003, pp. 96–101.
- [15] VENGSARKAR A.M., LEMAIRE P.J., JUDKINS J.B., BHATIA V., ERDOGAN T., SIPE J.E., *Long-period fiber gratings as band-rejection filters*, Journal of Lightwave Technology **14**(1), 1996, pp. 58–65.

*Received August 29, 2005  
in revised form September 27, 2005*